PHOTOMASK

BACUS—The international technical group of SPIE dedicated to the advancement of photomask technology.

BACUS N • E • W • S

January 2010
Volume 26, Issue 1

Second Place Best Paper Award

Source-Mask co-Optimization (SMO) using Level Set Methods

Vikram Tolani, Peter Hu, Danping Peng, Tom Cecil, Robert Sinn, Linyong (Leo) Pang, and Bob Gleason, Luminescent Technologies, Inc., Palo Alto, CA, USA 94303

ABSTRACT

Masks computed by use of Inverse Lithography Technology (ILT) are being increasingly used in 32nm and below nodes for their significantly better litho performance outperforming model-based OPC.[1,2] This technique poses the design of photomasks as an inverse problem and then solves for the optimal photomask using rigorous mathematical approach.[3,4] One such approach is the level set based method[5] wherein a level set function φ(x,y) is made to represent the contour of the mask. The zero level set φ(x,y)=0 then represents the actual mask at a given instance. The same level-set technique has now been extended to determine the most optimized source φ(p,q) for a given target or mask. Cooptimization of both the source and mask is a natural extension of optimizing the mask alone in ILT. The same cost function, say maximizing DOF, which is used to compute the ILT mask can be used for the source optimization as well.

This approach enables accurate and fast computation of the optimized source and mask for given set of patterns and also utilizes running on a distributed computing environment.

In this paper, the level set based SMO approach will be first validated on simple contact array patterns and then extended to the optimization of sample 22nm logic contact design patterns, including array, SRAM and random logic. The effect of using different emphasis in defining the cost function will also be studied.

1. Introduction

As optical lithography extends to sub-0.35 k1 regime, and minimum design pitches to sub-100nm, it becomes increasingly challenging to maintain reasonable lithographic process window (e.g., Depth Of Focus or DOF) and MEEF (Mask Error Enhancement Factor) using conventional source and mask conditions. Illumination sources that typically work for the sub-100nm pitches also result in more pronounced forbidden pitches and sub-optimal performance in real SRAM and random logic patterns. This leaves litho and design teams with the choice of either using highly restricted design rules and conventional source-mask conditions or using RET techniques such as ILT, Source-Mask Optimization (SMO), etc. to try and get the desired litho performance across a broader set of design patterns, with minimal restrictions to design rules.

When performing SMO, it is crucial to co-optimize both the source and mask, and not just have the source based on the target design patterns. This is because the optimized mask patterns are expected to have SRAFs (Sub-Resolution Assist Features) which play an important role in providing the required process window for looser pitches thereby not requiring the source to adjust for such looser pitches.

Furthermore, typical litho performance desired in terms of DOF and MEEF are often found to compete with each other. In such instances, it becomes important for a robust SMO method to provide for trade-offs between these competing metrics.

Continues on page 3.

SPIE

Editorial

All the Best – Have a Happy and Prosperous New Year

Warren Montgomery, 2009-2010 BACUS President

I would like to take this opportunity to wish everyone the best for the New Year!

BACUS had a pretty good year, in spite of the slowly recovering economy in 2009. The 2009 Photomask Symposium was a success, though the submissions and attendance was down, resulting in a 3 day conference instead of the usual 4 days. Not surprising in light of the economic environment. Larry Zurbrick was last year's conference chair and he did a masterful job guiding the 2009 Photomask conference; thanks Larry!

Last year, the BACUS Steering Committee made a few changes to the Photomask Symposium. A new and exciting technology was introduced to BACUS; Patterned Media (thanks to Brian Grenon). Wolf Staud changed the format of the Thursday Special Session (typically called the Friday Special Session) to a 'bar' format; the new format was well received. Finally, the SPIE team introduced a new twist in place of the usual BACUS banquet. The food was presented in a buffet style and there was a very nice audio/visual show. Many attendees have welcomed the change (a special thanks to Pat Wight, Ed Lake, and Brian Thomas.)

As we prepare for 2010, the Steering committee leadership has changed. Brian Grenon was replaced as President by Warren Montgomery. Wolf Staud has been selected as the Vice President replacing John Whittey, and Artur Balasinski is the Secretary replacing yours truly. Let me take this opportunity to thank the prior Executive Committee and offer a good luck wish to the new committee!

This year's Photomask Symposium will be held September 13 through 17 in Monterey, CA. The Co-chairs for the Symposium are Warren Montgomery of CNSE (Assigned to SEMATECH) and Wilhelm Maurer of Infineon Technologies AG. On behalf of the BACUS Committees, I encourage you to participate in the 2010 Photomask Symposium. Personally, it is my hope to see each and every one of you at the Photomask Symposium in the upcoming New Year.

Happy Holidays!

BACUS N • E • W • S

BACUS News is published monthly by SPIE for BACUS, the international technical group of SPIE dedicated to the advancement of photomask technology.

Managing Editor/Graphics Linda DeLano
Advertising Teresa Roles-Meier
BACUS Technical Group Manager Pat Wight

SPIE

P.O. Box 10, Bellingham, WA 98227-0010 USA
Tel: +1 360 676 3290 or +1 888 504 8171
Fax: +1 360 647 1445
SPIE.org
customerservice@spie.org

Continued from cover.

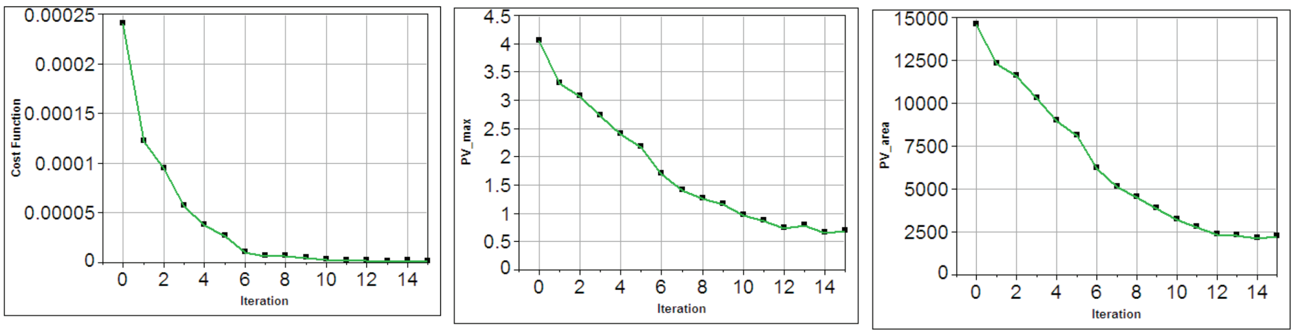

Figure 1a. Cost Function and PV trends through source-mask iterations for the 60/160 staggered contact case.

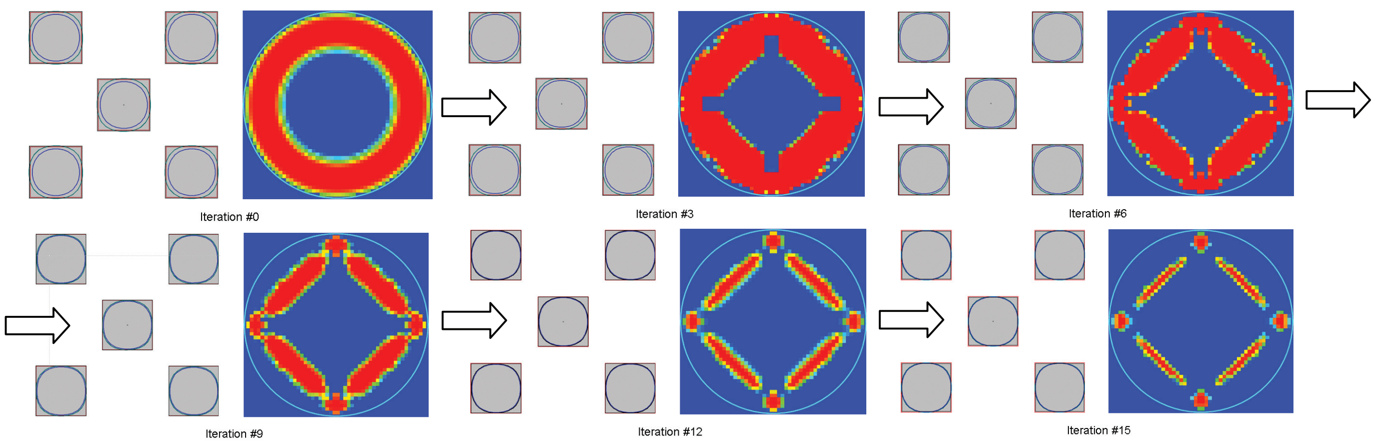

Figure 1b. Sequence of Mask (grey), Nominal (green), 75nm defocus (blue) image contours and Source through source-mask iterations for the 60/160 staggered contact case.

2. Level Set Based SMO

2.1 Cost Function in SMO

In any optimization problem, the Cost Function or Objective Function refers to the function that needs to be minimized or maximized. In case of the source-mask optimization problem, the cost function can be defined in different ways. For example, the optimization could be posed to maximize the contrast or ILS (Image Log Slope), of the limiting contrast design. The contrast approach generally works only for certain regular arrays, and furthermore, does not really represent lithographic performance in terms of actual DOF or exposure latitude or MEEF. Likewise, the optimization could be posed to maximize or minimize one of these metrics, however it would not then consider the other competing metrics during the optimization.

In Inverse Lithography using level set methods, the cost function is defined in terms of weighted dose/defocus/mask-bias images that need to be optimized. So for example, if both DOF and MEEF need to be optimized, then these images could be defined as certain dose/defocus, say ±50nm defocus/±3.5% dose, and certain mask-bias, say ±0.5nm. Furthermore, these images can be weighted depending on their relative importance to the user. In this way, any desired lithographic performance metric (DOF, EL, MEEF, ILS, PV or Process Variation) can be expressed in terms of the corresponding combination of dose/defocus/mask-bias images. If the exact images were not known, then certain guesstimates can be made for the expected performances.

2.2 Formulation of Level Set based SMO

In level set methods, the cost function is formulated as a Hamiltonian H of the state variable φ. In Inverse Lithography, this is defined as the difference between the printed wafer image $I^{\varphi}(x,y)$ and target $T(x,y)$, squared and integrated over the wafer domain Ω

$$H(\varphi) = \int_{\Omega} |I^{\varphi}(x,y) - T(x,y)|^2 \, dxdy$$

For mask optimization, the functional φ is formulated as:

$\{(x,y) : \varphi(x,y) > 0\}$ for regions outside the mask, i.e., mask background or field

$\{(x,y) : \varphi(x,y) <= 0\}$ for regions inside the mask

Similarly, for source optimization, the functional φ is formulated as:

$\{(p,q) : \varphi(p,q) > 0\}$ for regions where light pixels are OFF

$\{(p,q) : \varphi(p,q) < 0\}$ for regions where light pixels are ON

Continues on page 4.

Continued from page 3.

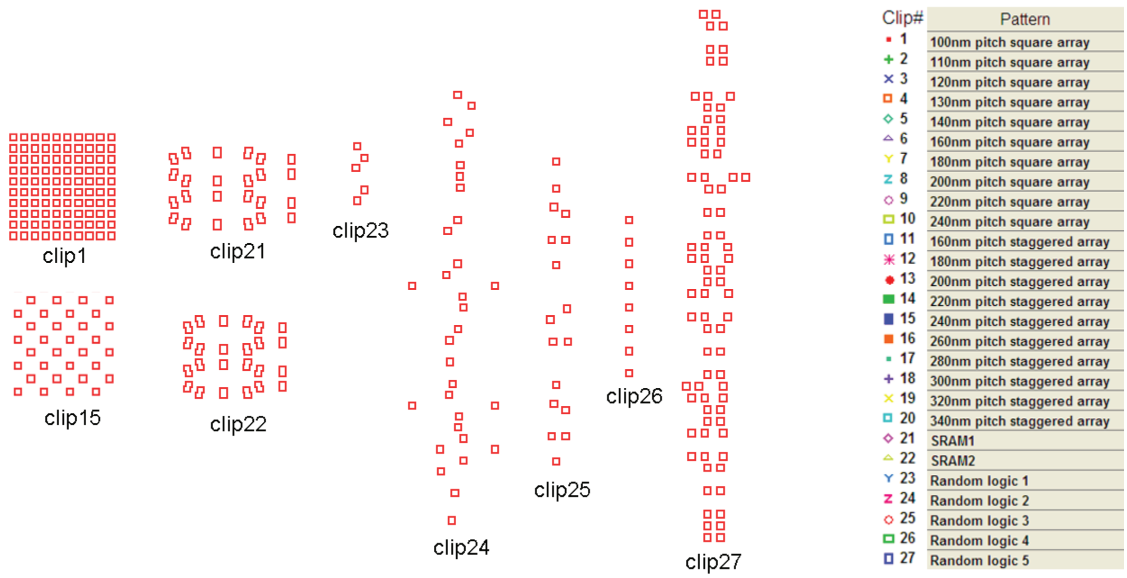

Figure 2. Sample design patterns of the 22nm logic contact design case.

The Hamiltonian H(φ) is then minimized using the gradient flow method.

2.3 Optimization flow during Level Set based SMO

The optimization process starts with an approximate source, say S_0. This could be a simple parameterized source such as annular, quasar, etc. Next, the optimization cost function is setup consisting of the desired images that need to be worked on and the initial ILT mask M_0 is computed for this initial source S_0. The flow then proceeds through iterative S_iM_i optimizations, always utilizing the recently generated $S_{i-1}M_{i-1}$ to finally converge on the optimal source-mask condition.

2.4 Validation on Simple Contact Array

Consider a staggered array of contacts of CD 60nm, and pitch 160nm. Assume water-based XY polarized illumination. Consider two images that need to be optimized – nominal and 75nm defocus, and include these in both the level set cost function and in the computation of PV images. As mentioned in 2.3, the optimization is started with a simple annular source (0.6 in/0.98 out) and then proceeds through iterations of sequential mask-source optimization. Figure 1a below shows the cost function and PV trends through these iterations. As the optimization proceeds, the source-mask cost function is continuously driven down and stabilizes before the 15th iteration. As with the cost function, the max. PV and PV area also decreases with each source-mask iteration. Max. PV is the largest PV pixel around the target patterns and PV area is the integrated area in between the PV bandwidth. In this case, max. PV is then the largest distance between the Nominal and 75nm defocus images, and PV area is the area of the band in between these two contours. Figure 1b shows the sequence of changes in the Mask (grey), nominal (green) and 75nm defocus (blue) image contours and Source. As can be seen from the contours, with each iteration, the nominal and 75nm defocus images get closer together, indicative of the PV improvements.

The converged source shape shown in Figure 1b, corresponding to Iteration# 12-15 is typical of what would be expected for getting an optimum DOF on a 160nm staggered contact array at 1.35NA based on intersection of its 0, and ±1 diffraction orders. The results on this simple case therefore validate the implementation of the level set method for source-mask optimization.

3. Application to 22NM Logic Contact Design

3.1 22nm Logic Contact Layout

A typical logic contact layout includes certain array, SRAM, and random logic patterns. Consider a 22nm node square contact layout consisting of square arrays of pitch 100-240nm pitch, staggered arrays of pitch 160-340nm, two SRAM and 5 random logic patterns, as shown in Figure 2. The optimization does not include looser pitch arrays since, with application of ILT-based SRAFs, these are expected to definitely perform better than the limiting tighter pitch patterns. The target contact CD is 60nm, NA is 1.35, illumination polarization is XY and mask type is binary.

The SMO results presented below first show the optimization on array-only, and SRAM/random logic-only patterns, and then their performance when optimized all together, finally concluding with results when using different cost function emphasis. The default cost function emphasis and PV calculations are still based on the Nominal and 75nm defocus images.

3.2 SMO Results on 22nm Array-only patterns

Clip#1-20 represent array-only patterns, including square and staggered layout of the contacts. While optimizing these 20 clips together, the cost function for the optimization is the sum of the individual clip cost functions. As can be seen in Figure 3a, during the optimization, this grouped cost function is driven

Continues on page 6.

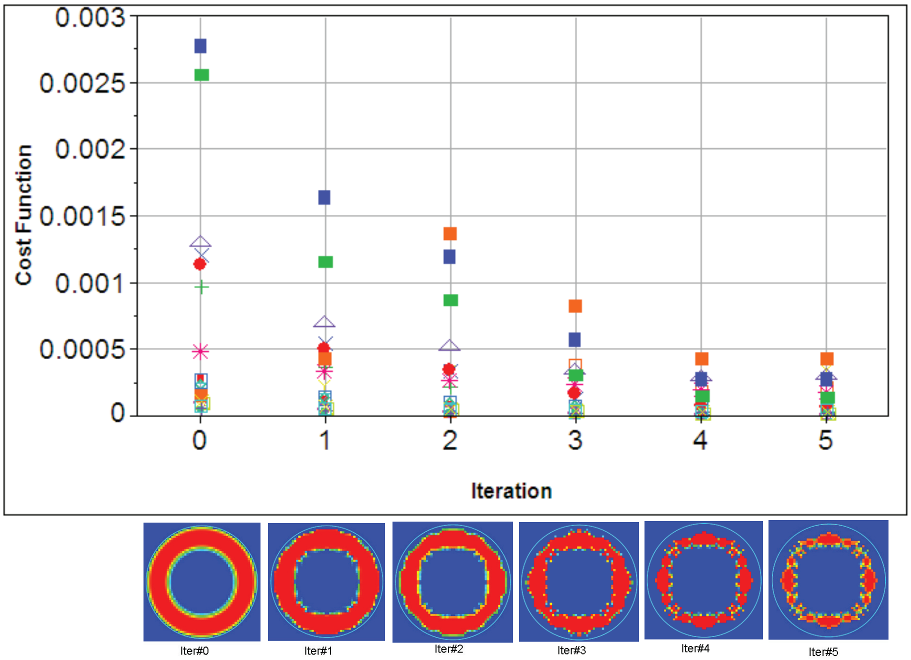

Figure 3a. Cost Function trends and optimized Source images through iterations for the optimization of the array-only patterns.

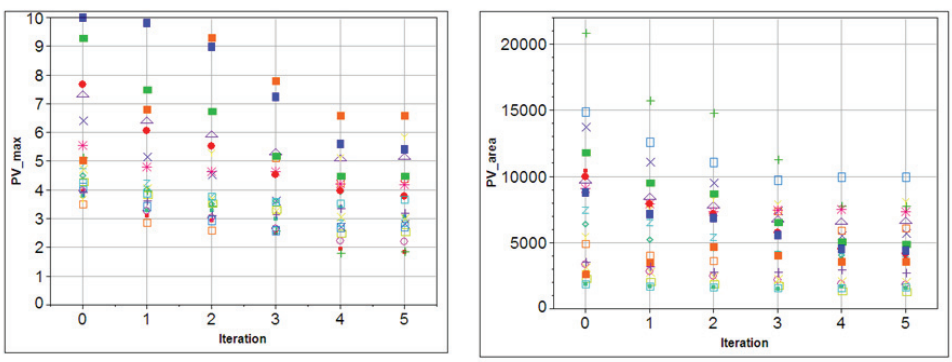

Figure 3b. PV trends through iterations for the optimization of the array-only patterns.

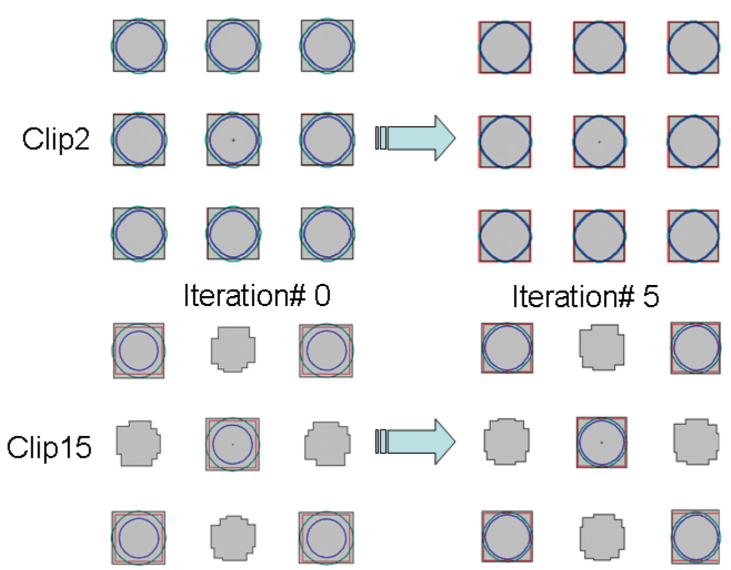

Figure 3c. Mask (grey), Nominal (green), 75nm defocus (blue) image contours for sample clips during the array-only SMO.

Continued from page 4.

down. While this sum performance is improved, it is interesting to note that some clips, for example clip#16 (orange square in Figure 3a) may actually have their cost functions increase during the optimization. In this case, clip#16 starts with a lower cost function value but then steadily increases in the first 2 iterations quickly becoming the limiting cost function but thereby also having a larger contribution to the grouped cost function. As a result, it then decreases as the source-mask iterations progress. The optimization converges after 5 iterations. Furthermore, it is interesting to note that the source images in Figure 3a are X/Y symmetric (i.e., 8-fold or D4 symmetric) since the array patterns are also X/Y symmetric. Figure 3b has the max. PV and PV area trends for all the clips, showing overall PV performance improving with each iteration, with the largest max. PV being 6.7nm for clip#16. Figure 3c shows examples of some of the limiting cases with the Mask (grey), nominal (green) and 75nm defocus (blue) image contours. Corresponding to PV improvements, the width between the nominal and 75nm defocus contours can be seen decreasing.

3.3 SMO Results on 22nm SRAM/Logic-only patterns

The SRAM and Logic patterns are in Clip#21-27. Similar to the optimization for the arrays, Figures 4a,4b,4c show the cost function, PV trends and sample mask and image contours through the source-mask iterations for the SRAM and random logic-only pattern optimization. It can be seen that the cost function contribution of clip#27 is the largest. This is partly because this clip has the most # of contacts as can be seen from Figure 2 and partly because it has contacts in some of the critical geometry limiting PV as seen in Figure 4b. The largest max. PV is 6nm for this clip#27. The optimized source in this case is not X/Y symmetric since the SRAM and Logic patterns are not X/Y symmetric.

3.4 SMO Results on all 22nm Array/SRAM/random Logic patterns

When the optimization includes all 27 clips of array, SRAM, and random logic patterns, the cost function, source, and PV trends with each source-mask iteration are shown in Figures 5a and 5b. It can be seen that the worst max. PV for the array patterns here is 7nm, and SRAM/random logic patterns is 6.5nm, both up from 6.7nm and 6.0nm respectively obtained when the array-only and SRAM/random logic-only patterns were optimized. Thus, as can be expected, the level set based SMO shows better (or same in other cases) source-mask performance when a subset of patterns are optimized than when all patterns are optimized together.

3.5 Using Different SMO Cost Function Emphasis

In the results presented above, the emphasis in the cost function was to minimize the deviation of the nominal and 75nm defocus images from the target design pattern. This emphasis can be easily adapted to user-specific requirements, as mentioned in 2.1. Suppose that besides defocus there is also emphasis in reducing MEEF. In that case, in addition to the existing nominal and defocus images, one would add ±0.5nm or ±1nm mask bias images into the cost function and rerun the level set based optimization. Figure 6a shows the cost function trends and final source solution for each of the three cost function cases. Figure 6b shows the corresponding PV and MEEF performance of the optimized source-mask solutions. As can be seen from the graphs, as the user emphasis of mask bias increases from 0 to ±0.5nm to ±1nm, the overall MEEF of the resulting solutions come down but at some expense to increase in PV (and hence lower DOF). Such an analysis of PV and MEEF trends for solutions obtained by simply changing the cost function weighted images, gives the user a very good idea of the Process Window vs. MEEF trade-offs involved before finalizing on a SMO solution.

3.6 Runtime and other Features

Typical runtimes of SMO using level set method, usually converging within <15 iterations for 25-50 clips on a cluster of 64 or 112cpus is about 1-1.5days. Furthermore, the optimization can incorporate different constraints, including source constraints such as pupil filling ratio, maximum outer sigma, etc., and mask constraints such as MRC main feature, SRAM width/space and minimum SRAF areas. The optimization can also incorporate scanner aberration data in terms of Zernike coefficients (scalar aberrations) and/or Jones Pupil (vector aberrations).

4. Conclusions

In summary, the level set based ILT mask computation algorithms have been extended now to the cooptimization of both source and mask. The method has been validated and applied to 22nm logic design patterns to yield optimum source-mask solutions across all desired designs. Also, the robustness of the level set method has been demonstrated with regards to different user emphasis in the cost function thereby providing SMO solutions showing tradeoffs between often competing litho performance metrics of DOF and MEEF. In conclusion, this method of co-optimization is tremendously useful in sub-0.35 k1 lithography.

5. Acknowledgments

The authors would like to thank GLOBALFOUNDRIES Inc. for sharing their 22nm test patterns for this development work

6. References

[1] Pang, L., Xiao, G., Tolani, V., Hu, P., Cecil, T., Dam T., Baik, K. and Gleason, B., “Considering MEEF in inverse lithography technology (ILT) and source mask optimization (SMO)”, *Photomask Technology 2008*, **Proc. Vol. 7122** (2008).

[2] Kim, B.G., Suh S.S., Kim B.S., Tolani, V., Dai G., Irby D., Wang K., Xiao G., Kim, D., Baik, K., and Gleason, B., “Trade-off between Inverse Lithography Mask Complexity and Lithographic Performance”, JPM09-7379-57 (2009).

[3] Saleh, B.E.A. and Sayegh, S.I., “Reductions of errors of microphotographic reproductions by optical corrections of original masks”, *Optical Eng.,* **Vol. 20,** p. 781-784 (1981).

[4] Nashold, K.M. and Saleh, B.E.A., “Image construction through diffraction-limited high-contrast imaging systems: an iterative approach”, *J. Opt. Soc. Am. A,* **Vol. 2,** p. 635 (1985).

[5] Osher, S. and Fedkiw, R., “Level Set Methods and Dynamic Implicit Surfaces”, *Applied Mathematical Sciences,* **Vol. 153,** Springer-Verlag ISBN 0-397-95482-1 (2000).

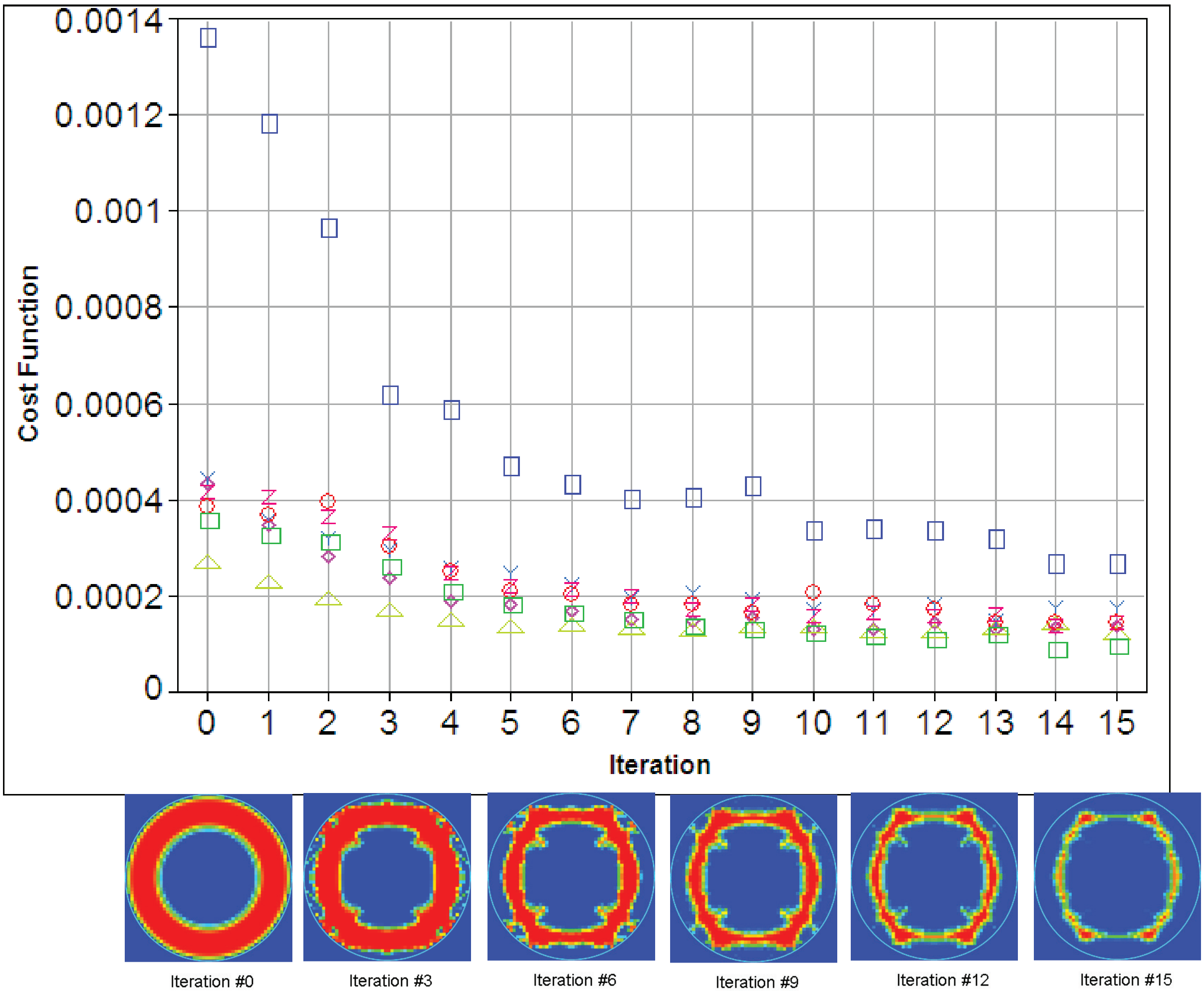

Figure 4a. Cost Function trends and optimized Source images through iterations for the optimization of the SRAM/random logic-only patterns.

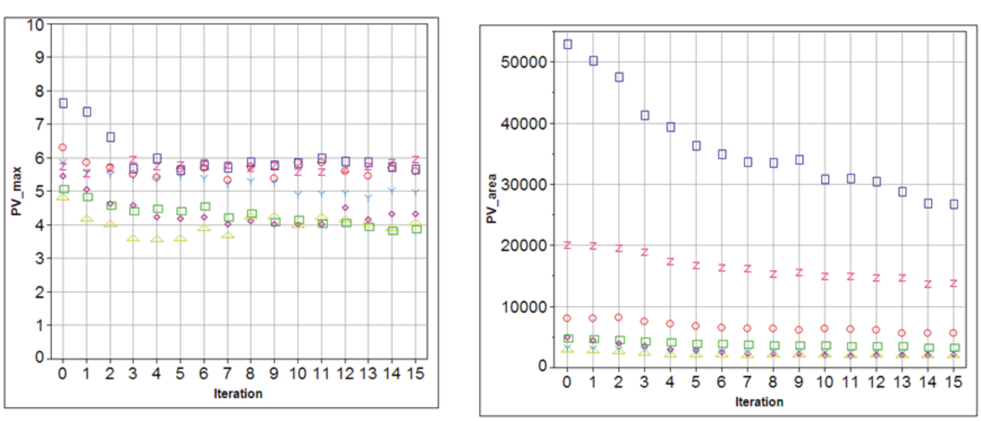

Figure 4b. PV trends through iterations for the optimization of the SRAM/random logic-only patterns.

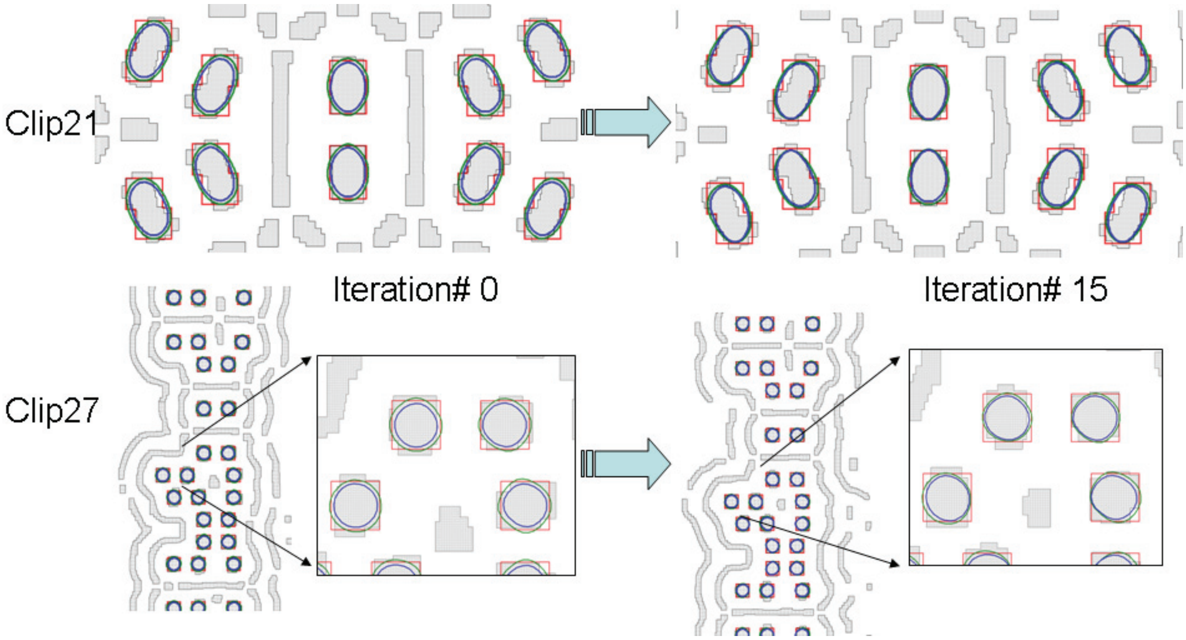

Figure 4c. Mask (grey), Nominal (green), 75nm defocus (blue) image contours for sample clips during the SRAM/random logic-only SMO.

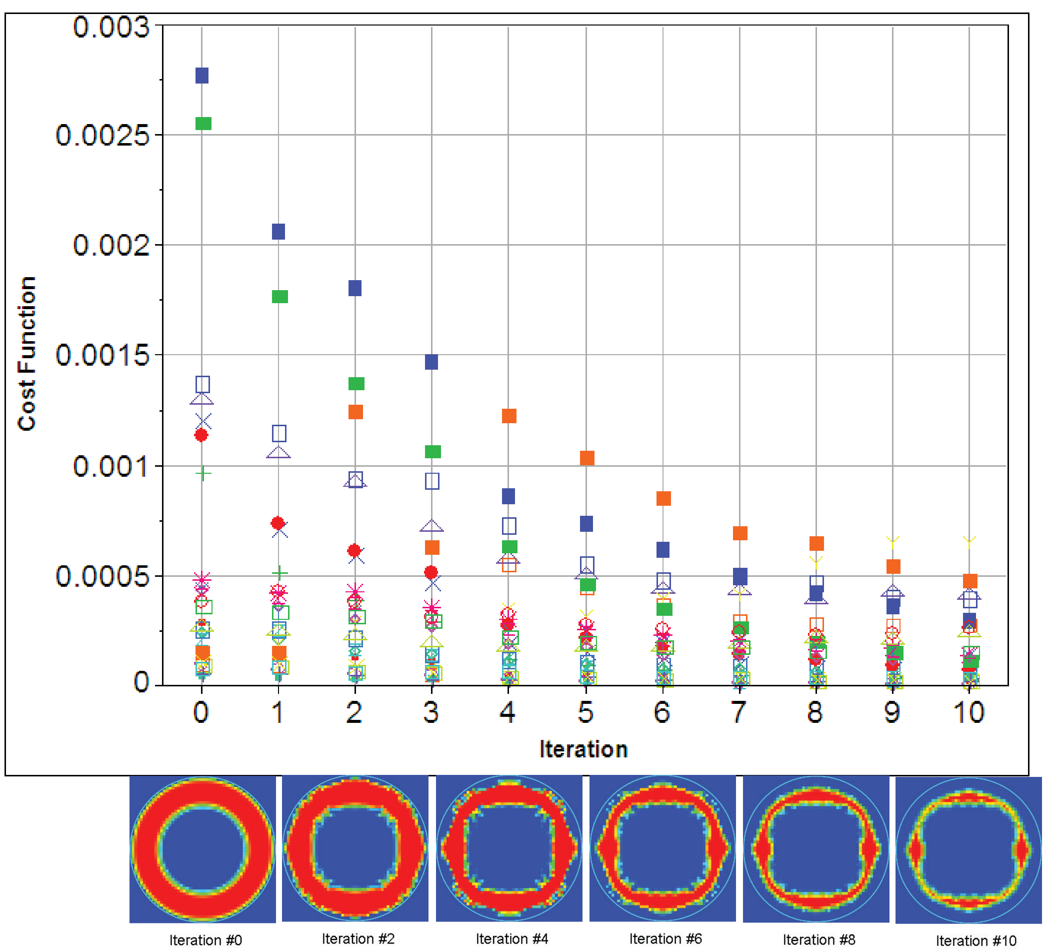

Figure 5a. Cost Function trends and optimized Source images through iterations for the optimization of all array, SRAM and random logic patterns.

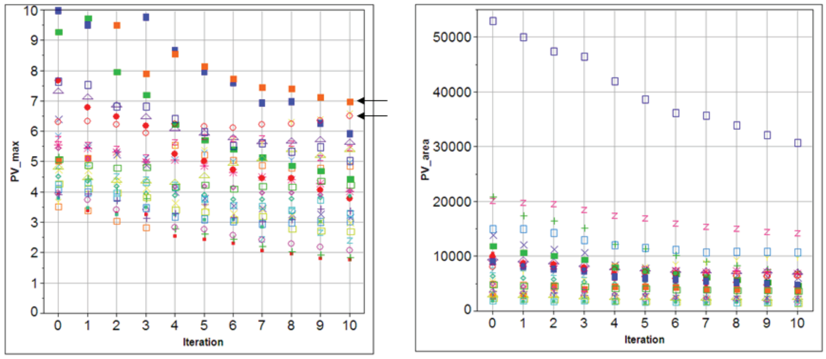

Figure 5b. PV trends through iterations for the optimization of all array, SRAM, and random logic patterns.

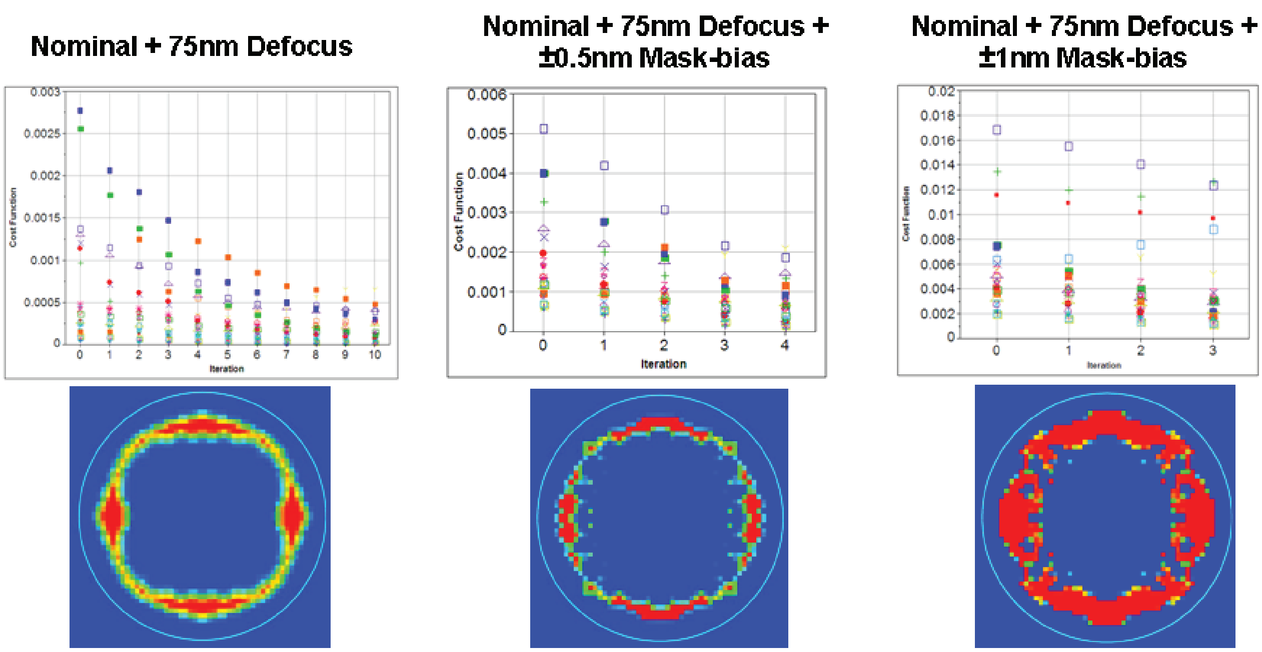

Figure 6a. Cost Function trends and optimized Source images for optimization on all patterns with different emphasis of defocus and mask-bias in the cost function.

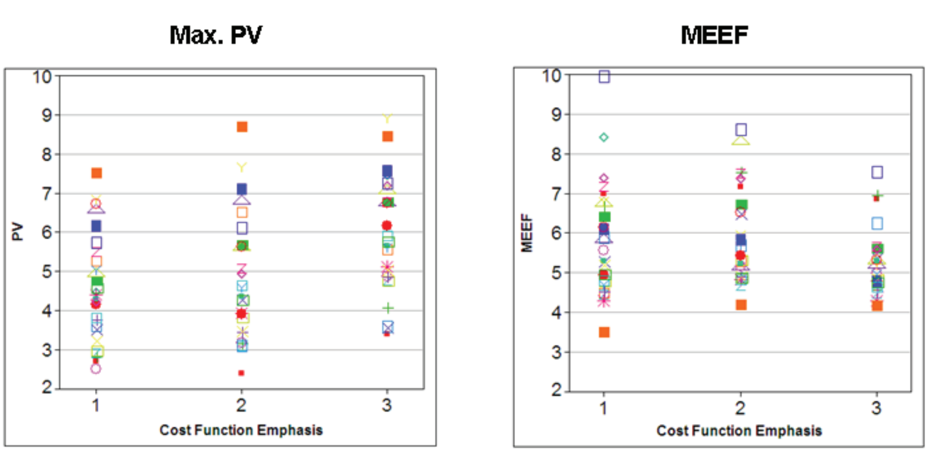

CF	Dose	Defocus	Mask-bias	CF	Dose	Defocus	Mask-bias
1	100%	75nm	0	1	100%	75nm	0
2	100%	75nm	0.5nm	2	100%	75nm	0.5nm
3	100%	75nm	1.0nm	3	100%	75nm	1.0nm

Figure 6b. PV and MEEF results of SMO solutions with different emphasis of defocus and mask-bias in the cost function.

Industry Briefs

Making E-beam direct write faster

By **Kiichi Sakamoto,** Advantest Corp., and **Aki Fujimura,** D2S Inc.

E-beam direct write (EbDW) lithography using character projection (CP) can enable maskless production for systems-on-chip (SoCs) at leading-edge technology nodes, with Design for e-beam (DFEB) improving the throughput of CP machines by the order of magnitude. Maskless CP EbDW eliminates mask costs for critical layers making it attractive for low-volume applications. While the variable-shaped beam (VSB) fractures the shapes into rectangles and triangles and the writing a single character takes several exposures, CP, in contrast, uses stencils to deploy complex characters on the second aperture of the e-beam machine in a single shot. Since EbDW write times are correlated with shot count, it determines the feasibility of maskless SoCs. For high EbDW throughput to make maskless SoCs practical, shot count must be reduced by an order of magnitude. SRAM core cells can require over 100 VSB shots, so a 100:1 reduction in shot count is possible with CP. Advantest F3000 machine specified a stencil mask containing 12 character block areas, each with 100 characters. Packed Stencil technology from D2S contains 20 character block areas, each with 220-280 characters.

The EbDW machine uses electrostatic deflection to switch between characters within the block area. To maintain accuracy, a certain radius of e-beam deflection is allowed, limiting the number of characters in a character block area. The deflection radius, however, is not what has dictates the standard 12 character blocks. This limitation is the result of a disconnect between design and manufacturing. Traditionally, a designer is not aware of what cells or layouts are easier for an EbDW to shoot, so the machine must be ready to project any character. The standard stencil mask is laid out in a grid pattern with pre-designated spots. The critical layers with the most time-consuming overhead (diffusion, poly, contact, metal 1, etc.) predominately consist of standard cells. Additionally, with pre-determined characters, a grid is unnecessary — characters can be arranged on the stencil to optimize their number. The stencil technology requires a design and manufacturing collaboration to allow more patterns to be shot as characters. The majority of the shot-count reduction comes from standard cells and SRAMs. A typical standard cell library may have 600 to over 1000 standard cells. A subset of the most usable and/or highest shot-count cells is chosen and any DFEB design can be synthesized. For any particular design, 100 characters per character block area may be nearly sufficient. The synthesis would insist on using a cell from the original library if needed for performance, power or area optimization. With 130 cells available, design can be optimized for shot count without sacrificing other quality-of-result metrics. EbDW has the potential to take all critical layers of SoC design directly to silicon without cost and delays of traditional mask production.

Photomasks Adapt to Shrinks, Require New Metrology

By **Alexander E. Braun,** Semiconductor International

Franklin Kalk, executive vice president and CTO at Toppan Photomasks Inc., considered the future of photomasks and lithography in light of the International Technology Roadmap for Semiconductors (ITRS). Kalk views critical dimension uniformity (CDU) influenced by the aerial image verification tool. The mask's resolution can't be done on a feature-by-feature basis or by random patterns. For memories with constant loading in the patterns, virtually all CD variation is over a long scale, either a side-to-side or a radial variation. For logic, pattern loads vary and one can see localized CD variation, not correctable except by process engineering or data manipulation. Mechanical repair hasn't kept pace with shrinks and E-beam will become more prevalent than the mechanical, nanochisel technique, especially with a move back to binary masks away from attenuated phase-shifting materials. The big issue for long-distance metrology is going from measuring fiducials arrayed around the pattern, or on the mask's far reaches, to in-die. In the past, customers preferred to live with the CD variation vs. pattern loading to avoid the extra cycle time due to data manipulation. Nowadays, they don't want that variation: In a model-based approach, all the features will be the right size. In the rule-based one, a simple set of rules a lookup table (pattern load, feature size) corrects for the required variation.

On some designs, mask pattern does not look like what will it be on the wafer. So when there are defects, it is hard to determine what to fix. Inspection tools must use aerial inspection, to generate an image that will have to be interpreted. It will be up to the repair tool not to just look at the defective pattern, but pair it to the original data and decide what and how much to fix. Luckily, repair tools are e-beam-based and have high resolution; but an electron isn't a photon. We must be careful not to be too ready to say we'll find defects with e-beam tools because we can compare it to the original data. The beam doesn't see what the photon saw. It'll be an interesting match between these two illumination sources.

Join the premier professional organization for mask makers and mask users!

About the BACUS Group

Founded in 1980 by a group of chrome blank users wanting a single voice to interact with suppliers, BACUS has grown to become the largest and most widely known forum for the exchange of technical information of interest to photomask and reticle makers. BACUS joined SPIE in January of 1991 to expand the exchange of information with mask makers around the world.

The group sponsors an informative monthly meeting and newsletter, BACUS News. The BACUS annual Photomask Technology Symposium covers photomask technology, photomask processes, lithography, materials and resists, phase shift masks, inspection and repair, metrology, and quality and manufacturing management.

Individual Membership Benefits include:

- Subscription to BACUS News (monthly)
- Complimentary Subscription *Semiconductor International* magazine
- Eligibility to hold office on BACUS Steering Committee

spie.org/bacushome

Corporate Membership Benefits include:

- One Voting Member in the SPIE General Membership
- Subscription to BACUS News (monthly)
- One online SPIE Journal Subscription
- Listed as a Corporate Member in the BACUS Monthly Newsletter

spie.org/bacushome

Calendar

2010

SPIE Advanced Lithography

21-26 February
San Jose Marriott and
San Jose Convention Center
San Jose, California, USA
spie.org/al

Late abstracts will be considered by the Chairs.

SPIE Photomask Technology

13-17 September
Monterey Marriott and
Monterey Conference Center
Monterey, California, USA
spie.org/pm

Abstract submissions will open early January.

SPIE Lithography Asia - Korea

Fall 2010
Location and Dates TBD - check **http://spie.org/la/** for updates.

Photomask Japan

13-15 April
Yokohama, Japan
http://www.photomask-japan.org/

You are invited to submit events of interest for this calendar. Please send to lindad@spie.org; alternatively, email or fax to SPIE.

SPIE is an international society advancing light-based technologies.

SPIE
International Headquarters
P.O. Box 10, Bellingham, WA 98227-0010 USA
Tel: +1 888 504 8171 or +1 360 676 3290
Fax: +1 360 647 1445
customerservice@spie.org • SPIE.org

Shipping Address
1000 20th St., Bellingham, WA 98225-6705 USA

SPIE Europe
2 Alexandra Gate, Ffordd Pengam, Cardiff,
CF24 2SA, UK
Tel: +44 29 20 89 4747
Fax: +44 29 20 89 4750
spieeurope@spieeurope.org • www.spieeurope.org